Secondary Ion Chemistry Mediated by Ozone and Acidic Organic Molecules in Iodide-adduct Chemical Ionization Mass Spectrometry

Wen Zhang and Haofei Zhang*

Department of Chemistry, University of California, Riverside in Riverside, California 92521, United States

*Corresponding Author: Haofei Zhang (haofei.zhang@ucr.edu)

ABSTRACT

Iodide-adduct chemical ionization mass spectrometry (I-CIMS) is a widely used technique in the atmospheric chemistry community to detect oxygenated volatile organic compounds (OVOCs) in real time. In this work, we report the occurrence of the secondary ion chemistry from interactions between a strong oxygen donor (such as O_3 and peracids) and acidic OVOCs (such as carboxylic acids and organic hydroperoxides) in the ion-molecule reaction (IMR) region of I-CIMS. Such interactions can lead to acidic organic molecules (HA or HB) clustering with $[IO]^-$ (e.g., $[HA+IO]^-$) and dimer adducts ($[A+B+I]^-$), in addition to the well-known iodide clusters ($[HA+I]^-$). This ion chemistry was probed using common chemical standards as well as the gas-phase oxidation products of α-pinene and isoprene in a flowtube reactor. The results show that the secondary ion chemistry can lead to misinterpretations of molecular compositions and distributions of the gas-phase products and an overestimation of the elemental O/C ratio overall. Nevertheless, the varying degrees of signal change in response to the secondary ion chemistry might be a clue to inform OVOCs' functionalities. Specifically, in the α-pinene ozonolysis system, the extents of ion signal reduction in the presence of additional acids in the IMR suggest that $C_9H_{14}O_4$ produced in the gas phase is a peracid, rather than the often-assumed pinic acid. Thus, we suggest that the potential application of the secondary ion chemistry to inform organic functionalities is promising, which could help better understand the molecular compositions of gas-phase OVOCs and the reaction mechanisms therein.

INTRODUCTION

Volatile organic compounds (VOCs) are ubiquitous in the atmosphere with substantial emissions from numerous biogenic and anthropogenic sources.[1-3] Reactive VOCs can be oxidized by oxidants in the atmosphere, producing oxygenated VOCs (OVOCs) which are a highly variable and complex class of organic mixtures with diverse functional groups, such as ketone, alcohol, carboxylic acid, hydroperoxide, etc.[4, 5] They play an important role as precursors to the formation of secondary organic aerosols (SOA) which have crucial impacts on the Earth's climate, air quality, and human health.[6-9] Understanding the compositions of OVOCs is thus imperative to gain significant insights into atmospheric chemistry and climate change.

Chemical ionization mass spectrometry (CIMS) has been a popular analytical technique to measure atmospheric VOCs and OVOCs in the past decades. It is well known for the high time-resolution (< 1 Hz), high sensitivity (ppt level), and the quantitative capability.[10-13] The soft ionization approach also allows for straightforward assignment of chemical formulas. Extensive studies in recent years applied a variety of reagent ions (e.g., I^-, CH_3COO^-, CF_3O^-, CO_3^-, SF_6^-, Br^-, and NO_3^- in the negative mode; H_3O^+, NO^+, O_2^+, NH_4^+, $C_6H_6^+$, and $C_2H_5OH^+$ in the positive mode) to selectively ionize different classes of organic compounds.[14-20] Iodide-adduct CIMS (I-CIMS) has been a favorite method among the various ionization schemes to detect a wide range of OVOCs due to its low selectivity.[21, 22] The detected iodide adducts are usually referred to as $[M+I]^-$, where M is considered as the molecular formula. Despite the wide usage of I-CIMS, potential interferences caused by, for example, secondary ion chemistry other than the iodide adducting have not been widely considered and examined.[13, 23, 24] Dörich et al. recently reported that the presence of strong oxygen donors such as O_3 and peracetic acid lead to biased detection of HNO_3 as NO_3^- using I-CIMS by the formation of $[IO_x]^-$.[25] It is yet unclear: (1) whether such

secondary ion chemistry in I-CIMS could also affect organic compounds; (2) whether the "M" in measured iodide adducts $[M+I]^-$ can all be interpreted as molecular formulas in the samples; (3) if any secondary ion chemistry occurs, how product quantification can be affected; and (4) how the secondary ion chemistry might be utilized to help identify products. To address these questions in this work, we examined the interactions of the strong oxygen donors (i.e., O_3, peracetic acid, and hydrogen peroxide) with organic species with diverse functionalities in I-CIMS using available OVOC chemical standards as well as produced mixtures from VOC oxidation experiments.

EXPERIMENTAL SECTION

I-CIMS. The I-CIMS used in this work is a commercial instrument (Aerodyne Research Inc.) with a time-of-flight mass spectrometer (TOFMS, $m/\Delta m \sim 5000$).[13] The I-CIMS instrument contains differentially pumped stages with a series of optics to achieve soft ionization and transmission of target molecules in the gas phase.[13, 21, 22] Defused CH_3I as a reagent source is introduced through a ^{210}Po alpha emitter into to the IMR chamber orthogonal to the sample flow to form charged iodide adducts with analytes under 100 – 110 mbar in the IMR, where the reaction time is ~ 0.1 s.[12, 13] The IMR is followed by a collisional dissociation chamber (CDC)[10, 11, 13] containing a segmented quadrupole where weakly bound ion-molecule clusters can dissociate into reagent ions and a neutral molecule with the changing electric strength. The CDC is followed by a second segmented quadrupole and a series of DC optics to guide, focus, and accelerate the primary beam into the TOFMS. The pressures in the two segmented quadrupoles are 4.8 (± 0.1) and 7.0 (± 0.2) × 10^{-3} mbar, respectively. The voltage difference (dV) between the two quadrupole regions can be tuned to control ion declustering.[21, 22] The operating dV is 4.8 V, determined by the tuning software (Thuner, v1.11) to optimize instrument sensitivity and resolving power. The

effective ion path length of the TOFMS is approximately 0.5 m to capture the ions under vacuum ($0.8 – 1.0 \times 10^{-6}$ mbar) by the detector with different detection time corresponding to different m/Q in the mass spectra.[10, 13, 20, 22] The TOFMS was operated over an m/Q range of 0-700 Th. All data analysis was done using Tofware (v3.2.0) running with Igor Pro (WaveMetrics, OR, USA).

Chemicals and Reagents. The following chemicals and reagents with purities and suppliers were used in the present study: formic acid (FA, 98% – 100%, LiChropur), acetic acid (AA, ≥99%, Sigma-Aldrich), propionic acid (PRA, 99%, Fisher), pyruvic acid (PYA, >97.0%, TCI), *cis*-pinonic acid (PIA, 98%, Sigma-Aldrich), peracetic acid (PAA, 32% wt.% in AA, Sigma-Aldrich), deuterated-4 acetic acid (dAA, 99.5%, CIL), acetone (99.7%, Fisher Chemical), glycerol (100%, J. T. Baker), propylene glycol (99%, Combi-Blocks), tert-butyl hydroperoxide (TBH, 70% aq. soln., Alfa Aesar), hydrogen peroxide (H_2O_2, 30% aq. soln., Fisher Chemical), α-pinene (98%, Acros Organics), and isoprene (99%, Alfa Aesar). Their structures and formulas are shown in the **Supporting Information** (**SI, Table S1**). None of the above reagents were further purified.

Secondary ion chemistry examined using chemical standards. All the above-mentioned chemical standards except α-pinene and isoprene were used to study the secondary ion chemistry in the I-CIMS. They were introduced to the clean dry air flow (2.1 L min^{-1}, provided by a clean air generator by Aadco Inc.) into the IMR inlet by a syringe pump (Chemyx Inc.), either individually or as mixtures. In addition, O_3 was added to the sampling air flow by an O_3 generator (Ozone Solution Inc.) at 0 – 200 ppb which is a typical range for lab experiments and polluted atmosphere.[26, 27] The O_3 concentrations were measured by an O_3 analyzer (Thermo Environmental Instruments, 49C). Alternatively, H_2O_2 and PAA as oxygen donors were hypothesized to play a similar role as O_3 in the secondary ion chemistry (if any). Thus, in two separate sets of experiments, H_2O_2 or PAA was injected using a separate syringe pump into the sampling air flow at varied

concentrations to interact with the other chemical standards in the IMR. The mixing time of O_3/H_2O_2/PAA with the organic standards before entering the IMR was ~ 0.2 s. Finally, we have also tested the effects of relative humidity (RH) and IMR pressure on the secondary ion chemistry using AA and O_3.

Gas-phase products from oxidation of α-pinene and isoprene. To examine the secondary ion chemistry with more realistic atmospherically relevant OVOCs, gas-phase oxidation experiments of two important VOCs, α-pinene and isoprene, by O_3 were conducted in a laminar flowtube reactor (Quartz, 110 cm long, 5.5 cm id., cone-shaped ends, volume ~ 2.1 L) at room temperature (~21 ℃). The experimental setup of VOCs oxidation is shown in **Scheme 1**. The residence times were 60 s and 70 s for the α-pinene and isoprene experiments, respectively. α-Pinene and isoprene were injected into the flowtube using a syringe pump. To minimize the influence of residual O_3 from the flowtube reactor on the secondary ion chemistry in the IMR, low initial O_3 concentrations (~ 20 ppb) and high VOC concentrations (14.7 ppm α-pinene and 68.0 ppm isoprene, respectively) were used. Under these experimental conditions, O_3 concentrations were estimated to be < 5 ppb at the exit of the flowtube reactor, based on the kinetic Master Chemical Mechanism (MCMv3.3.1) model (see **SI**, **Figure S1**).[28] At the exit of the flowtube, additional O_3 (~ 0.3 L min^{-1}, concentration measured by a second O_3 analyzer) was introduced to meet with the oxidation-derived OVOC mixtures (O_3 concentration after mixing ~ 0 – 200 ppb) and guided into the IMR. Because the VOC (e.g. α-pinene) ozonolysis products may contain oxygen donors themselves (i.e., peroxides and Criegee intermediates),[29-31] we added various acids (FA, AA, dAA, and PRA) into the IMR instead of H_2O_2 or PAA, with the goal to elucidate the oxygen donors in the OVOC products. Similar to the chemical standard experiments, the mixing

time between the oxidation products and the additionally injected O_3 or acids was ~ 0.2 s before entering the IMR. Thus, reactions during this mixing time are expected to be negligible.

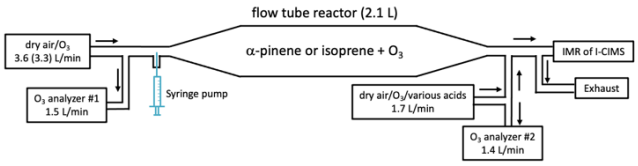

Scheme 1. The schematic diagram of the VOC oxidation experimental setup consisting of an injection system, a self-designed flowtube reactor and the I-CIMS. The flow rates of the various injection and sampling lines are illustrated.

RESULTS AND DISCUSSION

Observation and proposed mechanism for the secondary ion chemistry. To demonstrate the secondary ion chemistry in the I-CIMS IMR between different classes of organic compounds and oxygen donors, we performed experiments using a series of standard compounds with different functional groups. **Figure 1** presents the experimental results using a mixture of five carboxylic acids. The concentrations of the individual acids in the sampling air flow were in the range of 21 – 72 ppb. Upon the addition of O_3 (**Figure 1B**) or PAA (**Figure 1C**), the mass spectra clearly showed additional peaks, indicating their reactions with the acidic compounds. This is unexpected because these standard compounds do not contain C=C double bonds and should not react with O_3 or PAA on the short mixing timescale. Thus, we suggest that these new product ions were formed from secondary ion chemistry in the IMR. The detailed analysis of the I-CIMS mass spectra allowed us to elucidate the chemical formulas of the product ions, labeled in **Figure 1**. Apparently, the new product ions were iodide clusters with the formulas of $[HA+IO]^-$ and $[A+B+I]^-$ (HA and HB represent generic acids). The variations of the parent iodide clusters (i.e., $[HA+I]^-$) and the products ions with O_3 or PAA concentrations are displayed in **Figure 2A – B**,

which clearly show the formation of $[HA+IO]^-$ monomers and $[A+B+I]^-$ dimers as a function of IMR O_3 and PAA, along with the decreased parent ion intensities. We further examined the parent and product ions under declustering dV scans where iodide adducts dissociate into I^- and neutral molecules with increasing collisional energy (**Figure 2C**). The parent ions signals kept decreasing with increased dV, consistent with previous work.[22] However, $[HA+IO]^-$ and $[A+B+I]^-$ exhibited different extents of delayed dissociation with increased dV. Particularly, the $[A+B+I]^-$ dimers showed an increasing trend at dV from 5 to 10 V. We suggest that the observed delayed dissociation and even enhanced ion signals with dV increase are likely caused by the secondary ion chemistry. In a test with AA by varying the RH (< 2 – 80%) and IMR pressure (65 – 100 mbar), the secondary ion chemistry products were always present, which however, became more pronounced with higher RH but exhibited a decreasing trend as the IMR pressure dropped (**Figure 2D**).

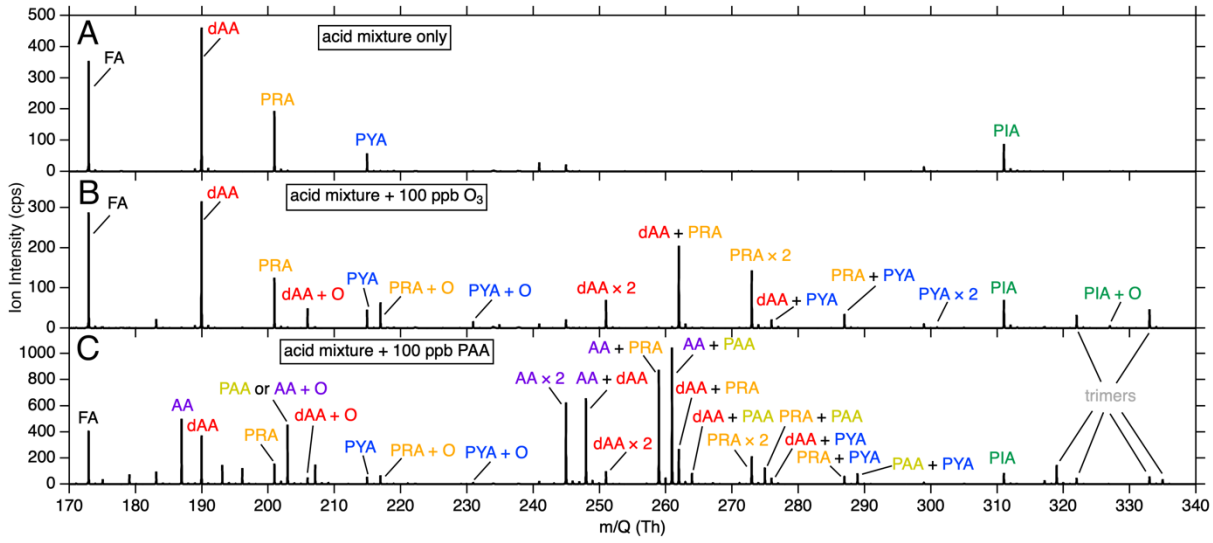

Figure 1. I-CIMS mass spectra of the acid mixture experiments: (A) the acid mixture only (B) in the presence of 100 ppb O_3 in the IMR, and (C) in the presence of 100 ppb PAA in the IMR. The I^- part of the ions are omitted in the labels for clarity. Note that the signal of dAA showed up at

m/Q 190 Th ($[CD_3COOH+I]^-$), resulting from a H/D exchange on the acid group. The signal of AA at m/Q 187 Th in (C) was from the impurity of PAA (32% wt.% in AA).

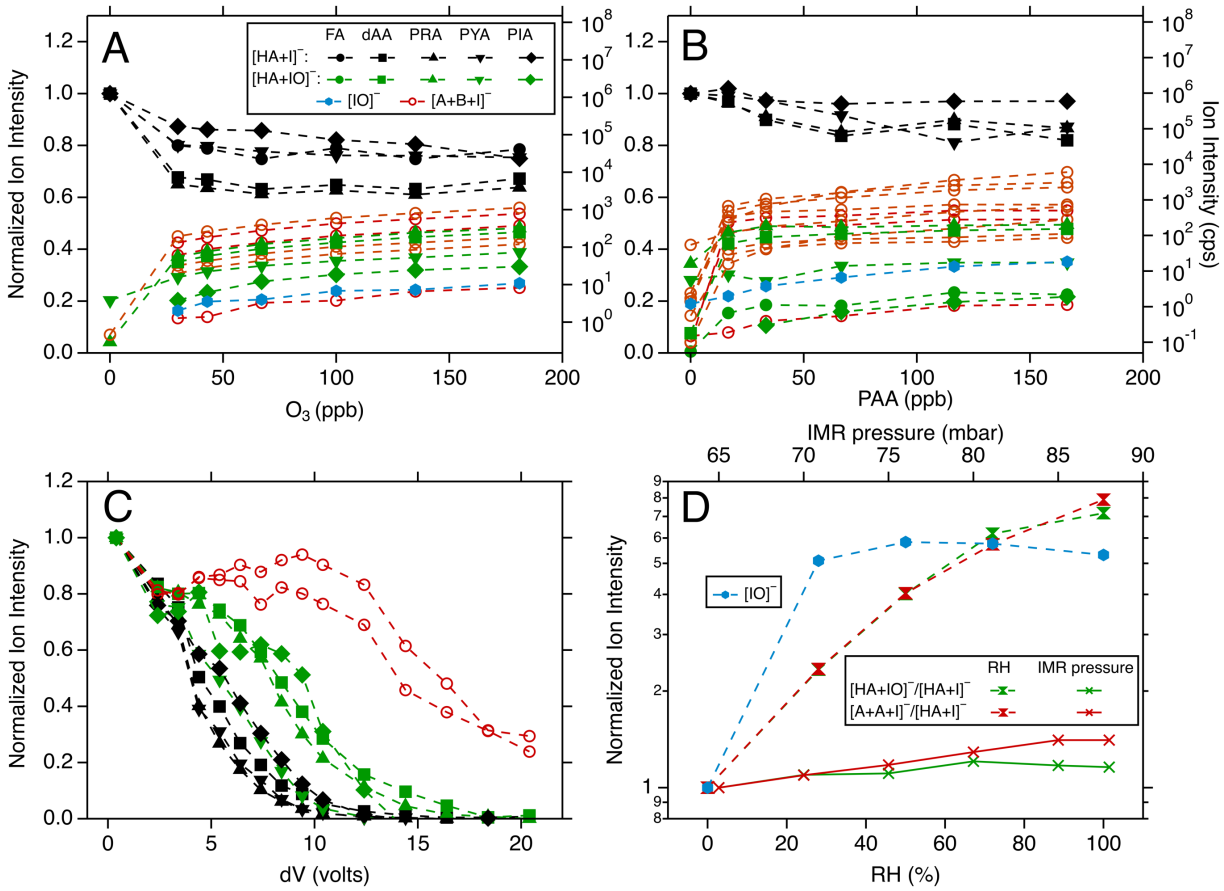

Figure 2. I-CIMS ion intensities of the parent ions ($[HA+I]^-$), $[HA+IO]^-$, and $[A+B+I]^-$ as a function of (A) O_3 concentration and (B) PAA concentration in the IMR. The parent ion signals are normalized for comparison. (C) Normalized ion intensities during the dV scans. (D) Normalized intensity ratios of $[HA+IO]^-$: $[HA+I]^-$ and $[A+A+I]^-$: $[HA+I]^-$ varied with different RH conditions (bottom *x*-axis) and IMR pressures (top *x*-axis). The signals of $[IO]^-$ are also shown in (A), (B), and (D). In (A) – (C), the dimer ions $[A+B+I]^-$ can be formed from the same or different monomeric acids and hence all the dimer ions are represented by red circle symbols.

In addition to the carboxylic acids, the experiments using TBH also showed sign of the secondary ion chemistry. Although TBH itself is not detectable by the I-CIMS, in the presence of O_3 and PAA, $[HA+IO]^-$ and $[A+B+I]^-$ were observed (**Figure S2**). In contrast, we did not observe the secondary ion chemistry in the experiments using the alcohols (propylene glycol and glycerol (**Figure S3**)) or acetone. Acetone itself is not detectable by I-CIMS similar to TBH, but the absence of products with O_3 or PAA suggests that it does not undergo the secondary ion chemistry. Interestingly, unlike O_3 and PAA, H_2O_2 does not induce the same secondary ion chemistry with the organic molecules, despite that it is also considered an oxygen donor like PAA. Moreover, when TBH was added with the organic acids, no additional products were observed, suggesting that simple hydroperoxides could not initiate the secondary ion chemistry as the oxygen donor. Based on these measurements, we propose a plausible mechanism of the observed secondary ion chemistry through the interactions of O_3 or peracids (the oxygen donors) with acidic organics (e.g., carboxylic acids and hydroperoxides) as follows:

$$I^- + O_3 \rightarrow [IO]^- + O_2 \quad (1)$$

$$I^- + RC(O)OOH \rightarrow [IO]^- + RC(O)OH \quad (2)$$

$$[H_2O+I]^- + O_3/RC(O)OOH \rightarrow [IO]^- + H_2O + O_2/RC(O)OH \quad (3)$$

$$[IO]^- + HA \rightarrow [HA+IO]^- \quad (4)$$

$$[IO]^- + HA \rightarrow A^- + HOI \quad (5)$$

$$[HA+IO]^- + HB \rightarrow [A+B+I]^- + H_2O \quad (6)$$

In this mechanism, O_3 and peracids (RC(O)OOH) initiate the secondary ion chemistry by reacting with I^- and produce $[IO]^-$ (Reactions (1) and (2)). The presence of water could promote the production of $[IO]^-$ (Reaction (3)) and hence the secondary ion chemistry (**Figure 2D**). This mechanism is further supported by the fact that $[IO]^-$ was observed to form in the presence of O_3

and PAA and promoted by RH (**Figure 2A, 2B, and 2D**). Following its formation, $[IO]^-$ can further cluster with acidic compounds (HA) to form $[HA+IO]^-$ (Reaction (4)). In a previous study by Iyer et al., dehydroxylation of PAA in the presence of I^- and H_2O was calculated to produce AA + $[IO]^-$ and $[AA-H]^-$ + HOI, with the latter combination having lower free energy than the former. This indirectly suggests that $[IO]^-$ might be able to deprotonate organic acids (Reaction (5)). Consistent with this reaction, the deprotonated organic acid ions are all found to be enhanced with O_3 and PAA (**Figure S4**). In addition, we propose that $[HA+IO]^-$ could cluster with another acidic molecule HB, and form the $[A+B+I]^-$ dimer clusters and water (Reaction (6)). As the declustering dV initially increased, the enhanced neutral molecules from cluster dissociation combine with $[HA+IO]^-$ to form $[A+B+I]^-$, explaining the temporal increase of the dimer clusters shown in **Figure 2C**. However, how A and B are bonded with each other and with iodide in $[A+B+I]^-$ remain puzzling and warrant future computational work. Further, the influence of the secondary ion chemistry on other organic functionalities is unknown so far due to the lack of standards detectable by I-CIMS. Small amounts of trimers were also observed (**Figure 1**), but their formation mechanism is not the focus of this work.

The effects of the secondary ion chemistry on molecular compositions of VOC oxidation products. Following the observation of the secondary ion chemistry using the chemical standards, we further performed oxidation experiments of α-pinene and isoprene in the flowtube reactor and used the I-CIMS to measure the OVOC products (**Scheme 1**), with the additional O_3 or acids at the IMR inlet. In the α-pinene ozonolysis experiments without additional O_3 or organic acids in the IMR (the control experiment), the gas-phase OVOC products are shown in **Figure 3A**, with the major peaks assigned to iodide adducts with $C_{8\text{-}10}H_{12\text{-}18}O_{3\text{-}6}$ with high-resolution peak fitting in the range of m/Q at 295 – 365 Th. These assigned formulas are consistent with prior

studies of α-pinene ozonolysis gas-phase products.[4, 32, 33] In the presence of additional O_3 in the IMR, most of the α-pinene derived OVOC products are affected by the secondary ion chemistry. With 197 ppb IMR O_3, the degrees of the variations of these products measured by I-CIMS are shown in the mass defect (δ_m) vs. m/Q plot in **Figure 4A** (mass spectrum shown in **Figure S5**). The combination of the formation of $[HA+IO]^-$ and the decreasing signal of $[HA+I]^-$ caused by the addition of IMR O_3 likely has led to the observed relative ion intensity changes. As a result, the intensities of many ions have largely increased, and some have reduced owing to the O_3-mediated secondary ion chemistry in the IMR. The dV scanning measurements also support these results. For example, the declustering profiles of $[C_{10}H_{16}O_4I]^-$ (a major product from α-pinene ozonolysis) show delayed declustering in the presence of IMR O_3 (**Figure 5A**). This observation is consistent with the results using chemical standards (**Figure 2C**), suggesting that the observed $[C_{10}H_{16}O_4I]^-$ was partially resulted from $[C_{10}H_{16}O_3+IO]^-$ when O_3 is present in the IMR. This is likely the case for many other product ions. However, the formation of the $[A+B+I]^-$ dimer ions is unclear with additional IMR O_3, owing to the low concentrations of the individual OVOC monomers and the fact that pre-existing dimers from α-pinene ozonolysis[34] could mask the identification of the formed $[A+B+I]^-$ dimer ions.

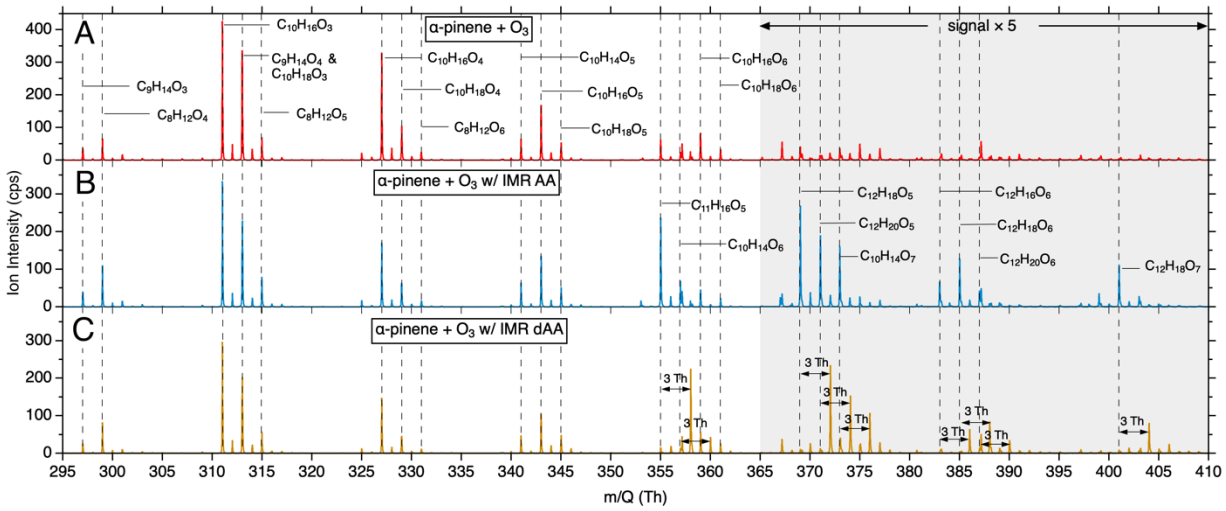

Figure 3. Mass spectra showing (A) the chemical composition of α-pinene ozonolysis monomer products (C_8 – C_{10}) in the absence of additional IMR O_3 or acids, (B) in the presence of IMR AA, and (C) in the presence of IMR dAA. Major products are labeled in the mass spectra, with the iodide part of the ion formulas omitted for simplification. The ion intensities are multiplied by 5 in the gray region. The vertical dashed lines are to guide the eye. The 3 Th mass shift of the same peaks between (B) and (C) was caused by the usage of dAA.

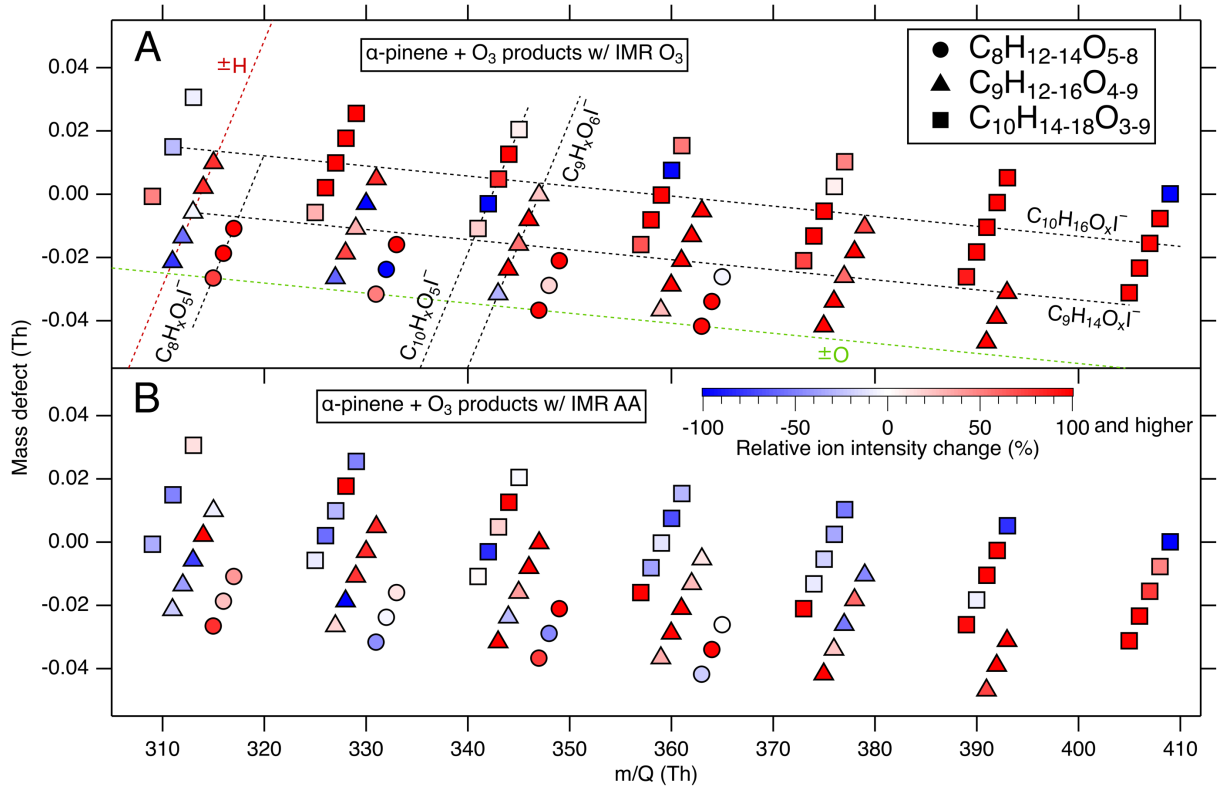

Figure 4. Mass defect plots of α-pinene ozonolysis C_8 – C_{10} products in the gas-phase (A) with IMR O_3 (B) and with IMR AA. The relative ion intensity change is marked by the color scheme in comparison to the products from the control experiment.

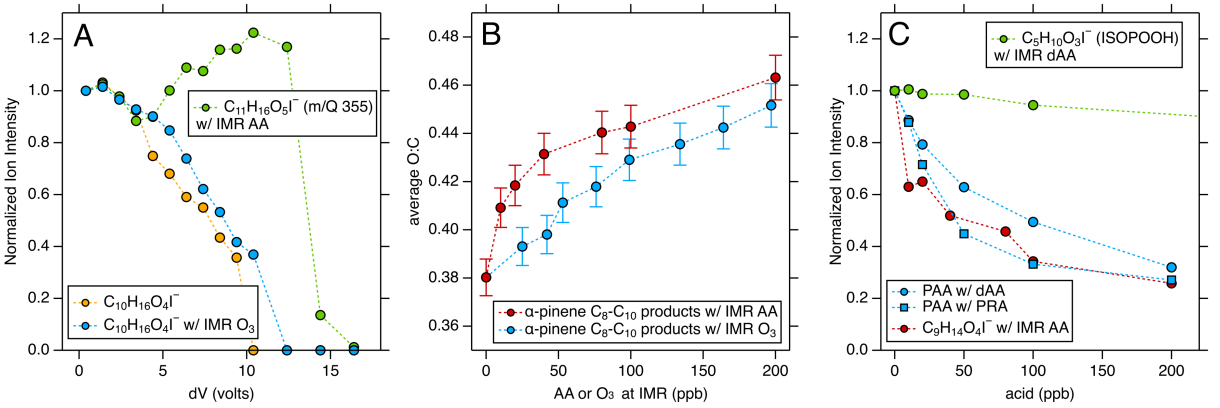

Figure 5. (A) Normalized ion intensities of $C_{10}H_{16}O_4I^-$ with and without IMR O_3 and $C_{11}H_{16}O_5I^-$ with IMR AA as a function of dV during the declustering scans. (B) The effect of the secondary

ion chemistry on the average O/C ratio of α-pinene ozonolysis major C_8 – C_{10} products. (C) The decreasing signals of PAA, ISOPOOH and $C_9H_{14}O_4I^-$ by varying degrees as the IMR acid concentration increases.

In comparison to the results with additional IMR O_3, a number of product ions showed up more prominently in the range of m/Q at 355 – 410 Th in the presence of IMR AA, which were determined as $C_{10\text{-}12}H_{14\text{-}20}O_{5\text{-}7}$ by the high-resolution peak fitting (**Figure 3B**). These observations indicate that the gaseous monomers with the formulas $C_XH_YO_Z$ have largely formed the $[A+B+I]^-$ dimer adducts ions with AA resulting in the apparent chemical formulas of $C_{X+2}H_{Y+2}O_{Z+2}$ (i.e., $[C_XH_YO_Z+C_2H_4O_2\text{-}2H+I]^-$). This is further confirmed by the m/Q shift of 3 Th in the mass spectra with dAA employed instead of AA (**Figure 3C**). From the experiments using the various chemical standards, we suggested that the formation of such $[A+B+I]^-$ dimer clusters require an oxygen donor and acidic organics. It should be noted that in these experiments, there was very little O_3 present in the IMR. Thus, we suggest that other oxygen donors naturally present in the α-pinene ozonolysis system such as peracids could be responsible for the occurrence of the secondary ion chemistry. In fact, α-pinene ozonolysis is known to produce substantial organic acids; therefore, the secondary ion chemistry could occur even without external interference with O_3 or acids. However, the extent of such ion chemistry is unassessable only by using I-CIMS. It is also worth studying whether other oxygen donors, such as Criegee intermediates, could play a similar role as O_3 and peracids in the studied ion chemistry since they are abundant intermediates in α-pinene ozonolysis. It is also highly likely that the OVOC products from α-pinene ozonolysis that showed the capacity of forming dimer clusters with additional IMR acids contain at least one acid, hydroperoxide or peracid functional group, as indicated by previous studies.[4] Moreover, the dimer

clusters' intensities in general correspond to their monomeric precursors, except for $[C_{11}H_{16}O_5I]^-$ whose precursor, $C_9H_{14}O_3$ has a low signal. The relatively poor sensitivity of I-CIMS to detect molecules with only two or three oxygen atoms may be partly responsible for this exception. Nonetheless, the declustering scan results shown in **Figure 5A** for $[C_{11}H_{16}O_5I]^-$ have clearly demonstrated that it is a dimer cluster from the secondary ion chemistry. On the other hand, more of the C_8 – C_{10} product intensities decrease with the addition of IMR AA, in contrast to the IMR O_3 experiments, as shown in **Figure 4B**. This is likely due to that the parent compound ($C_XH_YO_Z$) consumption by reacting with $[AA+IO]^-$ to form dimer clusters outcompetes the formation of $[C_XH_YO_{Z-1}+IO]^-$. We further examined the overall impacts of the secondary ion chemistry on the measured OVOC compositions using the elemental O/C ratios as a metric. As shown in **Figure 5B**, the average O/C ratios have increased by 15–20% as the concentrations of IMR O_3 or AA increased from 0 to 200 ppb. Therefore, the studied ion chemistry can lead to misinterpretation of molecular compositions by using I-CIMS, especially when both acidic molecules and oxygen donors are naturally present in the OVOC products.

The isoprene ozonolysis experiments showed only a few major peaks in the I-CIMS mass spectra (**Figure S6**), and thus is less focused in this work. Additionally, in comparison with the α-pinene experiments, isoprene oxidation is known to form less acidic products.[4, 33, 35-37] The only major product of interest is $[C_5H_{10}O_3I]^-$, which can be assigned to the isoprene hydroxy hydroperoxide (ISOPOOH) and the ISOPOOH-derived epoxydiol (IEPOX).[38] But based on the MCM kinetic simulations, under the short timescale in the flowtube experiments, ISOPOOH is expected to be 5 orders of magnitude more abundant than IEPOX (**Figure S1**). Thus, the observed $[C_5H_{10}O_3I]^-$ signals could be primarily contributed by ISOPOOH. With the additions of IMR O_3, we observed enhanced $[C_5H_{10}O_3+IO]^-$ (**Figure S7A**), consistent with the secondary ion chemistry.

With IMR dAA (dAA used instead of AA to avoid $[2AA\text{-}2H+I]^-$ confusion with $[C_5H_{10}O_3I]^-$ at m/Q 245), enhanced $[C_5H_{10}O_3+dAA\text{-}H\text{-}D+I]^-$ was also observed (**Figure S7B**), but the compositional change is to a lesser degree than α-pinene ozonolysis (**Figure 3**), likely owing to the smaller amount of oxygen donor in isoprene ozonolysis products. These results are consistent with the TBH standard measurements (**Figure S2**), suggesting that the secondary ion chemistry occurs for hydroperoxides which are slightly acidic.

The potential application of the secondary ion chemistry to inform functional groups and help elucidate chemical mechanisms. In the chemical standard experiments, we found that the addition of acids into the IMR can largely consume $[PAA+I]^-$. **Figure 5C** shows the normalized ion intensity of $[PAA+I]^-$ as a function of the concentration of IMR acids (dAA and PRA). With 200 ppb of carboxylic acids, approximately 60% of the initial PAA adduct signals ($[C_2H_4O_3I]^-$) were reduced due to the secondary ion chemistry under study. However, because we did not have another hydroperoxide standard observable by the I-CIMS available (TBH is not detectable by I-CIMS), it was unclear whether the observed PAA reduction is due only to the hydroperoxide or the entire peracid functionality. This question was addressed by the measurements of ISOPOOH ($[C_5H_{10}O_3I]^-$) in the isoprene ozonolysis experiment. The intensity of ISOPOOH decreased by a much smaller degree in the presence of IMR acids than that of the PAA (**Figure 5C**), indicating that the peracid functionality is crucial for the significant reduction. The dramatic difference between peracids vs. hydroperoxides also provides insights into the α-pinene ozonolysis products which decreased greatly with IMR acids (**Figure 4B**). In particular, the intensity of $[C_9H_{14}O_4I]^-$ in the α-pinene experiments dropped by a similar fraction to PAA, corresponding to the IMR acid (**Figure 5C**). The molecule $C_9H_{14}O_4$, a key product from α-pinene ozonolysis, is commonly known as pinic acid in the particle phase.[32, 33] Jenkin et al.[37] proposed a mechanism of the

formation of pinic acid from the isomerization of a C_9 acyloxy radical (**Figure 6**). In contrast, Ma and Marston[39] showed that pinic acid was enhanced by the addition of HO_2 radicals, suggesting that pinic acid could also be formed from perpinalic acid (a peracid) through intramolecular isomerization (**Figure 6**). In this work, the large drop of $[C_9H_{14}O_4I]^-$ in the presence of IMR acids in I-CIMS suggesting that the $C_9H_{14}O_4$ molecule in the gas phase is mostly likely a peracid (i.e., the perpinalic acid), in support for the Ma and Marston's work. It is possible that perpinalic acid undergoes further Baeyer-Villiger reactions[4] to further form pinic acid in the gas and/or particle phases. The investigation of the formation and structures of $C_9H_{14}O_4$ could be a focus in future experiments. Although the studied secondary ion chemistry from interactions of oxygen donors and acidic organics in I-CIMS can affect OVOC compositional interpretations, it likely has varying degrees of impact on different classes of organic compounds. Therefore, the potential application of I-CIMS secondary ion chemistry to inform functional groups is promising in forthcoming studies.

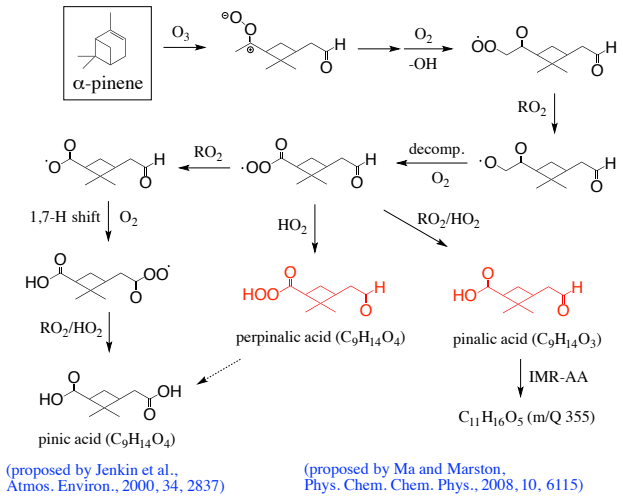

Figure 6. Proposed mechanism of the formation of $C_9H_{14}O_4$ in the gas phase which is identified as perpinalic acid.

CONCLUSIONS

In this work, we observed iodide clusters in the forms of $[HA+IO]^-$ and $[A+B+I]^-$ in I-CIMS, as a result of the secondary ion chemistry other than the well-known $[HA+I]^-$ clusters. A possible mechanism of the studied ion chemistry was proposed, through which the presence of O_3 or peracid as oxygen donors mediates the secondary ion chemistry with acidic organic molecules, including carboxylic acids, hydroperoxides, and peracids. In addition, we illustrated that the secondary ion chemistry in the IMR of I-CIMS could lead to misinterpretation of molecular compositions of oxidation products overall. The intensities of certain ions can be reduced by the formation of dimer clusters or enhanced from the secondary ion chemistry of the molecules with one fewer oxygen. As a result, the average O/C ratio of α-pinene ozonolysis products was increased by 15–20% due to the secondary ion chemistry with the addition of 200 ppb IMR O_3 or IMR acid. In the present study, we have also shown that the studied ion chemistry might be potentially applied to inform organic functionalities with the varying effect of the secondary ion chemistry. Thus, application of I-CIMS to identify different organic classes is promising, as we demonstrated that the oxidation product $C_9H_{14}O_4$ from α-pinene ozonolysis is first formed as perpinalic acid in the gas phase.

ASSOCIATED CONTEND

Supporting Information

Additional experimental mass spectra are provided in the Supporting Information.

AUTHOR INFORMATION

Corresponding Author

*E-mail: haofei.zhang@ucr.edu

Notes

The authors declare no competing financial interest.

ACKNOWLEDGMENTS

The work was supported by the start-up funding granted to H.Z. by University of California, Riverside. The chemical analysis was partially supported by National Science Foundation (CHE-2002413).

Reference

1. Goldstein, A. H.; Galbally, I. E., Known and unexplored organic constituents in the Earth's atmosphere. *Environ. Sci. Technol.* **2007,** *41* (5), 1514-1521
2. Hallquist, M.; Wenger, J. C.; Baltensperger, U.; Rudich, Y.; Simpson, D.; Claeys, M.; Dommen, J.; Donahue, N. M.; George, C.; Goldstein, A. H.; Hamilton, J. F.; Herrmann, H.; Hoffmann, T.; Iinuma, Y.; Jang, M.; Jenkin, M. E.; Jimenez, J. L.; Kiendler-Scharr, A.; Maenhaut, W.; McFiggans, G.; Mentel, T. F.; Monod, A.; Prévôt, A. S. H.; Seinfeld, J. H.; Surratt, J. D.; Szmigielski, R.; Wildt, J., The formation, properties and impact of secondary organic aerosol: current and emerging issues. *Atmos. Chem. Phys.* **2009,** *9* (14), 5155-5236.
3. De Gouw, J.; Jimenez, J. L., Organic Aerosols in the Earth's Atmosphere. *Environ. Sci. Technol.* **2009,** *43* (20), 7614-7618.
4. Claflin, M. S.; Krechmer, J. E.; Hu, W.; Jimenez, J. L.; Ziemann, P. J., Functional Group Composition of Secondary Organic Aerosol Formed from Ozonolysis of α-Pinene Under High VOC and Autoxidation Conditions. *ACS Earth Space Chem.* **2018,** *2* (11), 1196-1210.
5. Kroll, J. H.; Seinfeld, J. H., Chemistry of secondary organic aerosol: Formation and evolution of low-volatility organics in the atmosphere. *Atmos. Environ.* **2008,** *42* (16), 3593-3624.
6. Merikanto, J.; Spracklen, D. V.; Mann, G. W.; Pickering, S. J.; Carslaw, K. S., Impact of nucleation on global CCN. *Atmos. Chem. Phys.* **2009,** *9* (21), 8601-8616.
7. Dockery, D. W.; Pope, C. A.; Xu, X.; Spengler, J. D.; Ware, J. H.; Fay, M. E.; Ferris, B. G.; Speizer, F. E., An Association between Air Pollution and Mortality in Six U.S. Cities. *N. Engl. J. Med.* **1993,** *329* (24), 1753-1759.
8. Boucher, O.; Randall, D.; Artaxo, P.; Bretherton, C.; Feingold, G.; Forster, P.; Kerminen, V.-M.; Kondo, Y.; Liao, H.; Lohmann, U.; Rasch, P.; Satheesh, S. K.; Sherwood, S.; Stevens, B.; Zhang, X. Y. Clouds and Aerosols. *In Climate Change 2013: The Physical Science Basis. Contribution of Working Group I to the Fifth Assessment Report of the Intergovernmental Panel on Climate Change;* Stocker, T. F., Qin, D., Plattner, G.-K., Tignor, M., Allen, S. K., Boschung, J., Nauels, A., Xia, Y., Bex, V., Midgley, P. M., Eds.; Cambridge University Press: Cambridge, United Kingdom and New York, NY, USA, 2013.
9. Watson, J. G., Visibility: Science and Regulation. *J Air Waste Manag Assoc.* **2002,** *52* (6), 628-713.
10. Aljawhary, D.; Lee, A. K. Y.; Abbatt, J. P. D., High-resolution chemical ionization mass spectrometry (ToF-CIMS): application to study SOA composition and processing. *Atmos. Meas. Tech.* **2013,** *6* (11), 3211-3224.
11. Huey, L. G., Measurement of trace atmospheric species by chemical ionization mass spectrometry: Speciation of reactive nitrogen and future directions. *Mass Spectrom. Rev.* **2007,** *26* (2), 166-184.
12. Riva, M.; Brüggemann, M.; Li, D.; Perrier, S.; George, C.; Herrmann, H.; Berndt, T., Capability of CI-Orbitrap for Gas-Phase Analysis in Atmospheric Chemistry: A Comparison with the CI-APi-TOF Technique. *Anal. Chem.* **2020,** *92* (12), 8142-8150.
13. Bertram, T. H.; Kimmel, J. R.; Crisp, T. A.; Ryder, O. S.; Yatavelli, R. L. N.; Thornton, J. A.; Cubison, M. J.; Gonin, M.; Worsnop, D. R., A field-deployable, chemical ionization time-of-flight mass spectrometer. *Atmos. Meas. Tech.* **2011,** *4* (7), 1471-1479.
14. Breitenlechner, M.; Fischer, L.; Hainer, M.; Heinritzi, M.; Curtius, J.; Hansel, A., PTR3: An Instrument for Studying the Lifecycle of Reactive Organic Carbon in the Atmosphere. *Anal. Chem.* **2017,** *89* (11), 5824-5831.

15. Huey, L. G.; Hanson, D. R.; Howard, C. J., Reactions of SF6- and I- with Atmospheric Trace Gases. *J. Phys. Chem.* **1995,** *99* (14), 5001-5008.
16. Crounse, J. D.; Nielsen, L. B.; Jørgensen, S.; Kjaergaard, H. G.; Wennberg, P. O., Autoxidation of Organic Compounds in the Atmosphere. *J. Phys. Chem. Lett.* **2013,** *4* (20), 3513-3520.
17. Hammes, J.; Lutz, A.; Mentel, T.; Faxon, C.; Hallquist, M., Carboxylic acids from limonene oxidation by ozone and hydroxyl radicals: insights into mechanisms derived using a FIGAERO-CIMS. *Atmos. Chem. Phys.* **2019,** *19* (20), 13037-13052.
18. Laskin, J.; Laskin, A.; Nizkorodov, S. A., Mass Spectrometry Analysis in Atmospheric Chemistry. *Anal. Chem.* **2018,** *90* (1), 166-189.
19. Sanchez, J.; Tanner, D. J.; Chen, D.; Huey, L. G.; Ng, N. L., A new technique for the direct detection of HO2 radicals using bromide chemical ionization mass spectrometry (Br-CIMS): initial characterization. *Atmos. Meas. Tech.* **2016,** *9* (8), 3851-3861.
20. Canaval, E.; Hyttinen, N.; Schmidbauer, B.; Fischer, L.; Hansel, A., NH4+ Association and Proton Transfer Reactions With a Series of Organic Molecules. *Front. Chem.* **2019,** *7*, 191.
21. Lee, B. H.; Lopez-Hilfiker, F. D.; Mohr, C.; Kurtén, T.; Worsnop, D. R.; Thornton, J. A., An Iodide-Adduct High-Resolution Time-of-Flight Chemical-Ionization Mass Spectrometer: Application to Atmospheric Inorganic and Organic Compounds. *Environ. Sci. Technol.* **2014,** *48* (11), 6309-6317.
22. Lopez-Hilfiker, F. D.; Iyer, S.; Mohr, C.; Lee, B. H.; D'Ambro, E. L.; Kurtén, T.; Thornton, J. A., Constraining the sensitivity of iodide adduct chemical ionization mass spectrometry to multifunctional organic molecules using the collision limit and thermodynamic stability of iodide ion adducts. *Atmos. Meas. Tech.* **2016,** *9* (4), 1505-1512.
23. Smith, D.; McEwan, M. J.; Španěl, P., Understanding Gas Phase Ion Chemistry Is the Key to Reliable Selected Ion Flow Tube-Mass Spectrometry Analyses. *Anal. Chem.* **2020,** *92* (19), 12750-12762.
24. Iyer, S.; He, X.; Hyttinen, N.; Kurtén, T.; Rissanen, M. P., Computational and Experimental Investigation of the Detection of HO2 Radical and the Products of Its Reaction with Cyclohexene Ozonolysis Derived RO2 Radicals by an Iodide-Based Chemical Ionization Mass Spectrometer. *J. Phys. Chem. A* **2017,** *121* (36), 6778-6789.
25. Dörich, R.; Eger, P.; Lelieveld, J.; Crowley, J. N., Iodide-CIMS and m/z 62: The detection of HNO3 as NO3− in the presence of PAN, peracetic acid and O3. *Atmos. Meas. Tech. Discuss.* **2021,** *2021*, 1-26.
26. von Kuhlmann, R.; Lawrence, M. G.; Crutzen, P. J.; Rasch, P. J., A model for studies of tropospheric ozone and nonmethane hydrocarbons: Model description and ozone results. *J. Geophys. Res.: Atmos.* **2003,** *108* (D9), 4294.
27. Li, Q.; Su, G.; Li, C.; Liu, P.; Zhao, X.; Zhang, C.; Sun, X.; Mu, Y.; Wu, M.; Wang, Q.; Sun, B., An investigation into the role of VOCs in SOA and ozone production in Beijing, China. *Sci. Total Environ.* **2020,** *720*, 137536.
28. Jenkin, M. E.; Young, J. C.; Rickard, A. R., The MCM v3.3.1 degradation scheme for isoprene. *Atmos. Chem. Phys.* **2015,** *15* (20), 11433-11459.
29. Mentel, T. F.; Springer, M.; Ehn, M.; Kleist, E.; Pullinen, I.; Kurtén, T.; Rissanen, M.; Wahner, A.; Wildt, J., Formation of highly oxidized multifunctional compounds: autoxidation of peroxy radicals formed in the ozonolysis of alkenes – deduced from structure–product relationships. *Atmos. Chem. Phys.* **2015,** *15* (12), 6745-6765.

30. Docherty, K. S.; Wu, W.; Lim, Y. B.; Ziemann, P. J., Contributions of Organic Peroxides to Secondary Aerosol Formed from Reactions of Monoterpenes with O3. *Environ. Sci. Technol.* **2005,** *39* (11), 4049-4059.
31. Hiberty, P. C., Mechanism of ozonolysis. Ab initio study of the primary ozonide and its cleavage to the Criegee intermediate. *J. Am. Chem. Soc.* **1976,** *98* (20), 6088-6092.
32. Christoffersen, T. S.; Hjorth, J.; Horie, O.; Jensen, N. R.; Kotzias, D.; Molander, L. L.; Neeb, P.; Ruppert, L.; Winterhalter, R.; Virkkula, A.; Wirtz, K.; Larsen, B. R., cis-pinic acid, a possible precursor for organic aerosol formation from ozonolysis of α-pinene. *Atmos. Environ.* **1998,** *32* (10), 1657-1661.
33. Yan, M. A.; Russell, A. T.; Marston, G., Mechanisms for the formation of secondary organic aerosol components from the gas-phase ozonolysis of α-pinene. *Phys. Chem. Chem. Phys.* **2008,** *10* (29), 4294-4312.
34. Zhao, Y.; Thornton, J. A.; Pye, H. O. T., Quantitative constraints on autoxidation and dimer formation from direct probing of monoterpene-derived peroxy radical chemistry. *Proc. Natl. Acad. Sci. U.S.A.* **2018,** *115* (48), 12142-12147.
35. Kamens, R. M.; Gery, M. W.; Jeffries, H. E.; Jackson, M.; Cole, E. I., Ozone–isoprene reactions: Product formation and aerosol potential. *Int. J. Chem. Kinet.* **1982,** *14* (9), 955-975.
36. Sauer, F.; Schäfer, C.; Neeb, P.; Horie, O.; Moortgat, G. K., Formation of hydrogen peroxide in the ozonolysis of isoprene and simple alkenes under humid conditions. *Atmos. Environ.* **1999,** *33* (2), 229-241.
37. E. Jenkin, M.; Shallcross, D. E.; Harvey, J. N., Development and application of a possible mechanism for the generation of cis-pinic acid from the ozonolysis of α- and β-pinene. *Atmos. Environ.* **2000,** *34* (18), 2837-2850.
38. Paulot, F.; Crounse, J. D.; Kjaergaard, H. G.; Kürten, A.; St. Clair, J. M.; Seinfeld, J. H.; Wennberg, P. O., Unexpected Epoxide Formation in the Gas-Phase Photooxidation of Isoprene. *Science* **2009,** *325* (5941), 730-733.
39. Ma, Y.; Marston, G., Multifunctional acid formation from the gas-phase ozonolysis of β-pinene. *Phys. Chem. Chem. Phys.* **2008,** *10* (40), 6115-6126.

For Table of Contents Only